# Mosaic Activating Mutations in *FGFR1* Cause Encephalocraniocutaneous Lipomatosis

James T. Bennett,[1,2,18] Tiong Yang Tan,[3,18] Diana Alcantara,[4] Martine Tétrault,[5] Andrew E. Timms,[6] Dana Jensen,[2] Sarah Collins,[2] Malgorzata J.M. Nowaczyk,[7] Marjorie J. Lindhurst,[8] Katherine M. Christensen,[9] Stephen R. Braddock,[9] Heather Brandling-Bennett,[10] Raoul C.M. Hennekam,[11] Brian Chung,[12] Anna Lehman,[13] John Su,[14] SuYuen Ng,[14] David J. Amor,[3] University of Washington Center for Mendelian Genomics, Care4Rare Canada Consortium, Jacek Majewski,[5] Les G. Biesecker,[8] Kym M. Boycott,[15,19] William B. Dobyns,[1,2,16,19] Mark O'Driscoll,[4,19,*] Ute Moog,[17,19,*] and Laura M. McDonell[15,19]

Encephalocraniocutaneous lipomatosis (ECCL) is a sporadic condition characterized by ocular, cutaneous, and central nervous system anomalies. Key clinical features include a well-demarcated hairless fatty nevus on the scalp, benign ocular tumors, and central nervous system lipomas. Seizures, spasticity, and intellectual disability can be present, although affected individuals without seizures and with normal intellect have also been reported. Given the patchy and asymmetric nature of the malformations, ECCL has been hypothesized to be due to a post-zygotic, mosaic mutation. Despite phenotypic overlap with several other disorders associated with mutations in the RAS-MAPK and PI3K-AKT pathways, the molecular etiology of ECCL remains unknown. Using exome sequencing of DNA from multiple affected tissues from five unrelated individuals with ECCL, we identified two mosaic mutations, c.1638C>A (p.Asn546Lys) and c.1966A>G (p.Lys656Glu) within the tyrosine kinase domain of *FGFR1*, in two affected individuals each. These two residues are the most commonly mutated residues in *FGFR1* in human cancers and are associated primarily with CNS tumors. Targeted resequencing of *FGFR1* in multiple tissues from an independent cohort of individuals with ECCL identified one additional individual with a c.1638C>A (p.Asn546Lys) mutation in *FGFR1*. Functional studies of ECCL fibroblast cell lines show increased levels of phosphorylated FGFRs and phosphorylated FRS2, a direct substrate of FGFR1, as well as constitutive activation of RAS-MAPK signaling. In addition to identifying the molecular etiology of ECCL, our results support the emerging overlap between mosaic developmental disorders and tumorigenesis.

Congenital malformations featuring asymmetry, focal anomalies, or segmental overgrowth have long been hypothesized to be due to post-zygotic (mosaic) mutations.[1] Gene discovery for these disorders has been challenging due to the absence of familial recurrence, difficulty obtaining affected tissues, and the challenge of detecting low-frequency genetic variation. Encephalocraniocutaneous lipomatosis (ECCL; [MIM 613001]) is a sporadic neurocutaneous disorder characterized by patchy, asymmetric malformations and absence of familial recurrence.[2] Given this presentation, as well as an equal sex ratio and the occurrence of discordant monozygotic twins, ECCL has been hypothesized to be due to mosaic mutations.[3–5] ECCL is characterized by cutaneous, ocular, and central nervous system (CNS) abnormalities, and in the absence of known genetic cause, diagnosis has been based on the presence of characteristic clinical features.[2,6] The most characteristic skin anomaly in ECCL is nevus psiloliparus, a well-demarcated, alopecic fatty tissue nevus on the scalp seen in 80% of affected individuals.[2] Other dermatologic features include frontotemporal or zygomatic subcutaneous fatty lipomas, non-scarring alopecia, focal dermal hypoplasia or aplasia of the scalp, periocular skin tags, and pigmentary abnormalities following the lines of Blaschko. Choristomas of the eye (epibulbar dermoids or lipodermoids) are also frequent (80% of individuals with ECCL), and can be unilateral or bilateral.[2] Characteristic CNS features in ECCL include intracranial and intraspinal lipomas (61% of affected individuals), and less often cerebral asymmetry, arachnoid cysts, enlarged ventricles, and leptomeningeal angiomatosis.[7] A predisposition to low-grade gliomas has also been observed.[8–12] Seizures and

[1]Department of Pediatrics (Genetics), University of Washington, Seattle, WA 98195, USA; [2]Center for Integrative Brain Research, Seattle Children's Research Institute, Seattle, WA 98101, USA; [3]Victorian Clinical Genetics Services, Murdoch Children's Research Institute, Department of Paediatrics, University of Melbourne, Melbourne, VIC 3052, Australia; [4]Genome Damage and Stability Centre, University of Sussex, Brighton BN19RQ, UK; [5]Department of Human Genetics, McGill University, Montreal, QC H3A0G4 Canada; [6]Center for Developmental Biology and Regenerative Medicine, Seattle Children's Research Institute, Seattle, WA 98101, USA; [7]Department of Pathology and Molecular Medicine, McMaster University, Hamilton, ON L8S 4J9, Canada; [8]National Human Genome Research Institute, National Institutes of Health, Bethesda, MD 20892, USA; [9]Department of Pediatrics, Cardinal Glennon Children's Medical Center, St. Louis, MO 63104, USA; [10]Departments of Pediatrics and Medicine (Dermatology), University of Washington, Seattle, WA 98195, USA; [11]Department of Pediatrics, Academic Medical Centre, University of Amsterdam, 1105AZ Amsterdam, Netherlands; [12]Department of Paediatrics and Adolescent Medicine, Queen Mary Hospital, University of Hong Kong, 21 Sassoon Road, Hong Kong, China; [13]Department of Medical Genetics, University of British Columbia, Vancouver, BC V6H3N1, Canada; [14]Monash University, Eastern Health, Department of Dermatology, Box Hill, VIC 3128, Australia; [15]Children's Hospital of Eastern Ontario Research Institute, University of Ottawa, Ottawa, ON K1H5B2, Canada; [16]Department of Neurology, University of Washington, Seattle, WA 98195, USA; [17]Institute of Human Genetics, Heidelberg University, 69120 Heidelberg, Germany
[18]These authors contributed equally to this work
[19]These authors contributed equally to this work
*Correspondence: m.o-driscoll@sussex.ac.uk (M.O.), ute.moog@med.uni-heidelberg.de (U.M.)
http://dx.doi.org/10.1016/j.ajhg.2016.02.006. ©2016 by The American Society of Human Genetics. All rights reserved.

**Table 1. Clinical Features of 5 Individuals with ECCL in Whom an *FGFR1* Mutation Was Detected**

| | LR12-068 | LR13-278 | IN_0039 | NIH_183 | LR14-261 |
|---|---|---|---|---|---|
| *FGFR1* mutation | c.1966A>G (p.Lys656Glu) | c.1638C>A (p.Asn546Lys) | c.1638C>A (p.Asn546Lys) | c.1966A>G (p.Lys656Glu) | c.1638C>A (p.Asn546Lys) |
| Mutation discovery method | ES | ES | ES | ES | smMIP |
| Age at last assessment | 7 y | 15 y | 17 m | 2 y 8m | 5 y |
| Gender | M | M | M | M | F |
| Neurocognitive function | normal | delayed, in special skills class | normal | normal | normal |
| Seizures | no | yes | no | no | no |
| Intracranial lipomas | yes | yes | yes | no | yes |
| Spinal lipomas | no | not assessed | yes (T2/3 and L5/S1) | no | no |
| CNS Other | Pilomyxoid/ pilocytic astrocytoma WHO I | Tectal tumor, left temporal cortical dysplasia | no | Pilocytic/ pilomyxoid astrocytoma WHO II | no |
| Nevus psiloliparus | yes | yes | yes | yes | yes |
| Alopecia | yes | yes | yes | yes (right parietal) | yes |
| Subcutaneous lipoma | yes (fronto-temporal) | yes | yes (fronto-temporal) | yes (parietal) | yes |
| Focal scalp aplasia | yes | yes | yes | yes | no |
| Skin tags | yes (eyelid) | yes | yes | yes (right eyelid, anterior to right ear) | yes |
| Choristoma | yes (bilateral) | yes | yes (right) | no | yes |
| Coloboma | no | yes (left upper eyelid) | yes (left upper eyelid, iris and bilateral retinal) | no (but segmental iris heterochromia present) | no |
| Prior Publication | no | yes[59] | no | yes[8] | yes[60] |

Abbreviations are as follows: ES (exome sequencing) and mMIP (single molecule molecular inversion probes).

intellectual disability are common but normal intellect is seen in a third of affected individuals.[2] Skeletal manifestations include bone cysts and jaw tumors, such as odontomas, osteomas, and ossifying fibromas.[13] ECCL had been proposed to be a localized form of Proteus syndrome (MIM 176920), although diagnostic criteria suggest that the two conditions are clinically distinct.[2]

To identify the molecular etiology of ECCL, we performed exome sequencing (ES) on DNA samples from five unrelated ECCL probands (IN_0039, LR12-068, LR13-278, LR13-175, NIH_183). Written informed consent to participate in this study was obtained for each participant. This study was approved by ethics review boards at the Children's Hospital of Eastern Ontario, Seattle Children's Hospital, and the National Human Genome Research Institute. Clinical features of these affected individuals are described in Table 1 and highlighted in Figures 1A–1D. To maximize the likelihood of detecting low frequency, tissue-restricted mosaic variants, we sequenced DNA at high coverage (64-172X) from probands' affected and unaffected tissue where possible. ES was also performed on blood-derived DNA from parents of probands LR12-068, LR13-278, LR13-175, NIH_183, and from the unaffected monozygotic twin sibling of IN_0039. ES platforms and data analyses are detailed in Tables S1 and S2. Genomic alterations identified by ES were screened against variants in the NHLBI Exome Sequencing Project Exome Variant Server (EVS), the Exome Aggregation Consortium (ExAC), the NCBI database (dbSNP), and in-house variant databases. Variants inherited from a parent, or present in the unaffected twin in the case of IN_0039, were also filtered out.

Two rare missense variants, c.1638C>A (p.Asn546Lys) and c.1966A>G (p.Lys656Glu), located within the intracellular tyrosine kinase domain of *FGFR1* (NM_023110.2), were identified in four of the five probands (Figures 1E and 1F). In IN_0039, the affected proband of a monozygotic twin pair discordant for ECCL, the p.Asn546Lys substitution was identified in fibroblasts cultured from biopsies of both unaffected skin (23% alternate allele fraction, AAF) and a scalp lesion (33% AAF), but was absent (0/76 reads at this position) from the unaffected twin's blood. In individual LR13-278, the p.Asn546Lys substitution was identified in fibroblasts cultured from biopsies of unaffected skin (35% AAF), scalp nevus (42% AAF), and eyelid dermoid (54% AAF). In proband NIH_183, the p.Lys656Glu substitution was identified in fibroblasts cultured from a scalp lesion (45% AAF) but was not detected in blood. In proband LR12-068, the p.Lys656Glu substitution was identified in fibroblasts

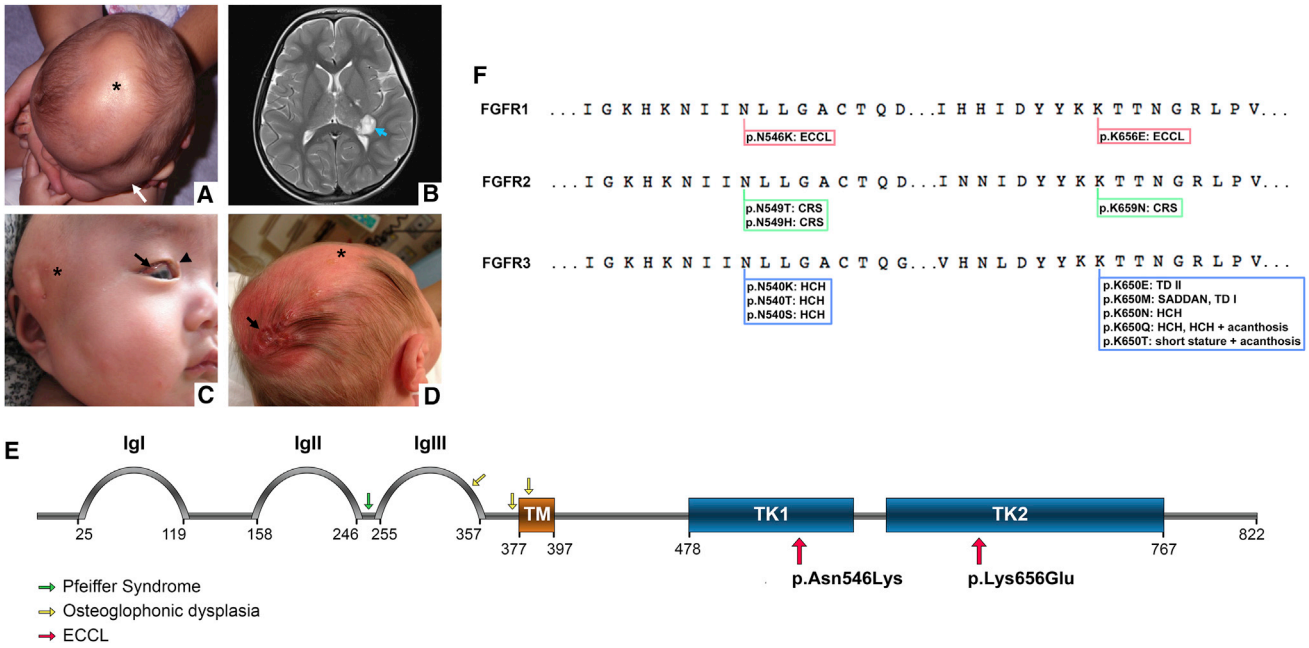


**Figure 1. Exome Sequencing Identifies *FGFR1* Mutations in Four Individuals with ECCL**

(A) Photograph of LR13-278, showing nevus psiloliparus (asterisk) and subcutaneous lipoma (arrow).

(B) Horizontal T2 MRI of LR12-068, showing pilocytic astrocytoma (light blue arrow) adjacent to posterior left lateral ventricle.

(C) Photograph of IN_0039, showing large subcutaneous lipoma (asterisk), epibulbar dermoid (arrow), and eyelid skin tag (arrowhead).

(D) Photograph of NIH_183 showing several regions of focal skin hypoplasia over vertex (arrow) and nevus psiloliparus anteriorly (asterisk).

(E) Protein structure of FGFR1. The three extracellular Ig-like domains, the transmembrane (TM) domain, and the two-part tyrosine kinase (TK1 and TK2) domain are shown. Locations of mutations for two other syndromes due to activating FGFR1 substitutions are shown: Pfeiffer syndrome in green (p.Pro252Arg) and osteoglophonic dysplasia in yellow (p.Asn330Ile, p.Tyr374Cys, and p.Cys381Arg). The two ECCL associated substitutions (p.Asn546Lys and p.Lys656Glu) are located in the cytoplasmic kinase domain.

(F) Amino acid sequences of FGFR1, 2, and 3 (P11362.3, P22607.1, P21802.1) were aligned using MUSCLE Alignment with the Geneious software.[55] In addition to the two ECCL substitutions in FGFR1, disorders associated with substitutions in paralogous amino acids in FGFR2[41,56] and FGFR3[26,34,57,58] are also shown. Abbreviations: CRS (craniosynostosis), HCH (hypochondroplasia), TD (thanatophoric dysplasia), and SADDAN (Severe Achondroplasia with Developmental Delay and Acanthosis Nigricans)

cultured from a scalp nevus (47% AAF), and from a pilocytic astrocytoma (32% AAF). In each case the *FGFR1* variant detected by exome sequencing was confirmed by Sanger sequencing. Neither of these two variants was present in EVS, ExAC, or dbSNP. No rare non-synonymous variants were identified in *FGFR1* in LR13-175. Coverage information for all eleven exome samples is included in Table S1. On the basis of finding four unrelated individuals with the same rare phenotype who shared one of two missense mutations in the same gene, we considered these variants in *FGFR1* to be pathogenic and causative of ECCL.

ES identified an additional *FGFR1* variant, c.1681G>A (p.Val561Met), in LR12-068, in 45/87 reads (45% AAF). This variant was present in the pilocytic astrocytoma but not in cultured skin fibroblasts (0/183 reads). Interestingly, this variant has been reported to confer resistance to lucitanib, a tyrosine kinase inhibitor (TKI) currently in phase II trials for FGFR-dependent tumors.[14,15] However, to mediate TKI resistance, the c.1681G>A (p.Val561Met) variant must be in *cis* with the primary *FGFR1* activating mutation.[14] We hypothesized that p.Val561Met was a second hit that arose during tumorigenesis in *cis* with this individual's primary *FGFR1* mutation, c.1966A>G (p.Lys656Glu). To test this, we subcloned DNA from the tumor sample. Briefly, a 1,408 basepair fragment containing both c.1681G>A and c.1966A>G was amplified from tumor DNA (primers listed in Table S3), subcloned into a plasmid (pCR2.1-TOPO, Life Technologies) using TOPO-TA cloning, and used to transform competent cells. Colonies containing the fragment were identified by PCR, expanded in liquid culture, and genotyped by Sanger sequencing. Of 20 clones isolated, 16 possessed neither variant, two possessed only the p.Lys656Glu variant, and two possessed both variants. These results suggest that the c.1681G>A (p.Val561Met) variant is in *cis* with the c.1966A>G (p.Lys656Glu) mutation, and possibly arose during tumorigenesis.

To facilitate the identification of mutations in *FGFR1* in additional individuals suspected of having ECCL, we developed an approach using single molecule Molecular Inversion Probes (smMIPs) because low-frequency mosaic mutations could be missed using conventional Sanger sequencing. smMIPs are an inexpensive and highly sensitive next generation sequencing method that have been reported to detect alleles present as low as 0.1%,[16] lower than the typical Sanger cutoff of 20%. smMIPs allows

independent molecular capture events to be distinguished, so that smMIP coverage is reported as independent reads, each of which represents an individual capture event.[16] Briefly, smMIPs were designed to capture all coding regions of *FGFR1* plus at least ten bases of flanking sequence. A pool of 47 smMIPs (sequences in Table S4) was hybridized with 120 ng of DNA from each sample in the cohort. Each smMIP contained a 5 nucleotide degenerate "molecular tag" used to distinguish independent molecular capture events. Sample-specific eight-base barcodes were introduced in subsequent PCR amplification steps, and pooled libraries were sequenced using a 101 cycle paired end protocol on an Illumina MiSeq. Reads were aligned to the human assembly hg19 using BWA, and GATK was used to refine local alignments and call variants (SNVs and indels). Reads with the same molecular barcode were collapsed to form independent reads, and we required the presence of a variant in three or more independent reads. We used smMIPs to screen multiple tissues from two probands (LR13-278 and IN_0039, see Table S5) with mutations in *FGFR1* detected by ES to determine the tissue distribution of the mutations. In LR13-278, the c.1638C>A (p.Asn546Lys) mutation was detected in DNA derived from fibroblasts (affected and unaffected skin), but was absent in blood- or saliva-derived DNA at a depth of 153 and 27 independent reads, respectively. This same mutation was detected in DNA derived from fibroblasts (affected skin) from individual IN_0039, but was absent in saliva, buccal swab, and blood-derived DNA, at depths of 114, 40, and 51 independent reads, respectively. At a depth of 27 independent reads, the smMIPs assay should be able to detect variants at a frequency as low as 11% (3/27). At a depth of 153 independent reads, the detection limit is as low as 2% (3/153). Because we were unable to detect *FGFR1* mutations in blood, saliva, or buccal swab derived DNA in two individuals with known mutations present at high levels (31%–55% AAF, see Table S5) in biopsied tissues, we suspect that the tissue distribution of *FGFR1* mutations in individuals with ECCL is skewed. Although it is possible that the *FGFR1* mutations are present in blood, saliva, or buccal swab at levels below our detection limit, these results suggest that the negative predictive value of *FGFR1* sequencing of these non-biopsied samples might be low for ECCL and that sequencing of skin-biopsy derived DNA will provide a higher diagnostic yield.

Using the same smMIP assay, we screened an independent cohort of four individuals with ECCL (LR14-261, LR04-090, LR09-120, and IN_0025, see Table S5) for whom tissue biopsy-derived DNA was available. We identified one additional individual (LR14-261) with the c.1636C>A (p.Asn546Lys) mutation in *FGFR1*, present at an allele fraction of 55% (110 of 199 independent reads) in DNA isolated from cultured fibroblasts from a scalp nevus, but was not detected in saliva (0/36 independent reads, see Table S5). Clinical details about this individual are listed in Table 1. No other *FGFR1* mutations were identified within any samples from these four individuals in which tissue biopsy-derived DNA was available. An additional group of three individuals (LR04-093, LR09-252, and LR14-210) with ECCL were screened using the smMIP assay, but for these three individuals only blood or saliva derived DNA was available (see Table S5). No additional *FGFR1* mutations were detected in this group, but since we did not have tissue biopsy-derived DNA available in this group, *FGFR1* mutations cannot be excluded. Clinical phenotypes of the individuals in which an *FGFR1* mutation was not detected were not different from those of individuals with an *FGFR1* mutation (data not shown). The number of independent reads at each of the two *FGFR1* mutation sites, for each tissue tested, is shown in Table S5.

Receptor tyrosine kinases (RTKs) regulate a wide range of complex biological functions including cell growth, differentiation, tissue patterning, and organogenesis.[17,18] Fibroblast growth factor receptors (FGFRs) represent an RTK subfamily comprising four homologous receptors encoded by four FGFR genes. The encoded proteins share a basic structure consisting of three extracellular ligand-binding immunoglobulin domains (IgI, IgII, IgIII) linked to a cytoplasmic protein kinase core (TK1 and TK2) via a single-pass transmembrane domain (TM) (Figures 1E and 2A).[19] The two recurrent FGFR1 substitutions are located within the cytoplasmic kinase core (Figures 1E and 1F). FGFRs function by binding their respective ligands and heparan accessory molecules to induce dimerization and conformational changes.[17,20] Following ligand binding, *trans*-phosphorylation of the cytoplasmic domains between dimer pairs releases *cis*-autoinhibition and enables catalytic kinase activity.[20–22] Phosphorylation of additional tyrosine sites in the kinase domain creates high affinity binding sites for proteins containing phosphotyrosine binding (PTB) domains and Src-homology 2 domains.[21] Catalytically active receptors initiate intracellular signaling through several pathways, including the RAS-MAPK network (Figure 2A), resulting in phosphorylation of downstream targets such as ERK1, ERK2, and C-RAF (HUGO gene names are *MAPK3*, *MAPK1*, and *RAF1*, respectively).

To determine the effect of ECCL mutations on FGFR activity, we conducted Western blot analysis of whole cell extracts from several fibroblast lines derived from LR13-278, who harbors the p.Asn546Lys substitution. Using antibodies that detect phosphorylation of FGFR1-4 on Tyr653 and Tyr654 (pFGFR-Y653/Y654), we observed spontaneously elevated levels of phosphorylated FGFRs in exponentially growing fibroblasts derived from the skin, eyelid, and scalp of LR13-278, compared to wild-type (WT) cells (Figure 2B). We next examined signal transduction in these cells following prolonged serum deprivation, compared to exponentially growing cells. WT fibroblasts showed the expected reduction in phosphorylation of FGFR (Figure 2C) and ERK1/2 phosphorylation (pERK1/2-T202/Y204) upon serum starvation (Figure 2C). In contrast, fibroblasts from LR13-278 exhibited elevated phosphorylation of FGFR and ERK1/2

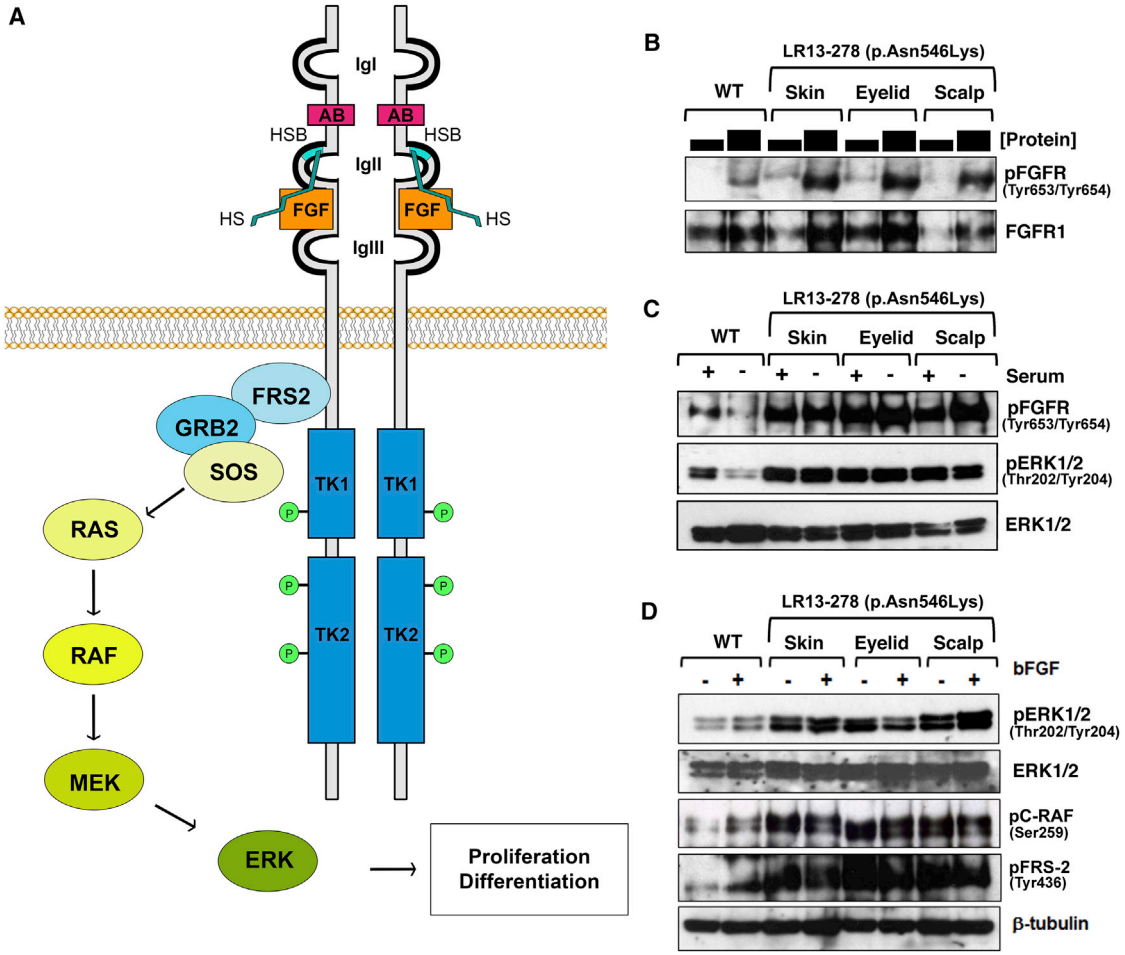


**Figure 2. Hyperphosphorylation of FGFR and RAS-MAPK Activation in an Individual with ECCL Due to p.Asn546Lys Substitution**
(A) Ligand and heparan-sulfate binding induces FGFR dimerization and conformational changes followed by *trans*-phosphorylation and activation of the cytoplasmic kinase domain. Phosphorylation of additional tyrosine sites in the kinase domain creates high affinity binding sites for downstream effector proteins such as FRS2, which recruits GRB2 and initiates RAS-MAPK signaling. The three extracellular Ig-like domains, the acid box (AB), heparan-sulfate (HS), heparan-sulfate binding site (HSB), fibroblast growth factor (FGF), and the two-part tyrosine kinase (TK1 and TK2) domain are shown.
(B) Differing amounts of whole-cell extract (WCE) from exponentially growing wild-type (WT) and ECCL fibroblasts derived from various tissues from LR13-278 were probed for FGFR-phosphorylation using pan-FGFR phosphorylation antibodies (pFGFR-Tyr653/Tyr654).
(C) WCE was prepared from exponentially growing cells (+ serum) and from cells that were serum starved for 72 hr (− serum) from wild-type (WT) fibroblasts and from various tissues from LR13-278. These were blotted using antibodies to detect pan-FGFR transphosphorylation and ERK1/2 phosphorylation.
(D) All fibroblasts were serum starved for 72 hr and then either untreated (−) or treated (+) with bFGF (10 nM for 15 min). WCE from wild-type (WT) and LR13-278 fibroblasts from various tissues were blotted to detect ERK1/2 and C-RAF phosphorylation and also for FRS2 phosphorylation. All antibodies were obtained from Cell Signaling Technology: anti-pFGFR-Tyr653/Tyr654 (Cat #3471S), anti-FGFR-1 (Cat #9740), anti-pFRS2-Tyr463 (Cat #3861S), anti-pERK1/2-Thr202/Tyr204 (Cat #9101S), anti-ERK1/2 (Cat #4695S), and anti-pC-RAF-Ser259 (Cat #9421).

compared to WT in the presence or absence of serum (Figure 2C). Similar results were observed in fibroblasts derived from the thigh and scalp of IN_0039 (data not shown). Finally, we examined FGFR-dependent signal transduction in LR13-278 fibroblasts in response to acute treatment with recombinant basic fibroblast growth factor (bFGF) following prolonged serum deprivation. WT fibroblasts treated with bFGF showed elevated levels of phosphorylated ERK1/2 and C-RAF, another RAS-pathway effector (Figure 2D). In contrast, fibroblasts from LR13-278 showed elevated levels of phosphorylated ERK1/2 and C-RAF even in the absence of bFGF stimulation (Figure 2D), suggesting ligand-independent activation of FGFR signaling. Because phosphorylated ERK1/2 and C-RAF can reflect increased activity of a variety of RTKs, we also examined FRS2, whose activating phosphorylation is mainly FGFR-dependent.[23] Similar to ERK1/2 and C-RAF, phosphorylated FRS2 is increased by bFGF stimulation in WT fibroblasts, but in LR13-278 elevated levels of phosphorylated FRS2 are present even in the absence of bFGF stimulation (Figure 2D). Collectively, these results demonstrate elevated autophosphorylation of FGFRs, the

FGFR-dependent substrate FRS2, and the RAS-pathway components C-RAF and ERK1/2, in multiple proband-derived fibroblasts with the p.Asn546Lys substitution (Figures 2B–2D and data not shown). A proband-derived fibroblast line harboring the p.Lys656Glu substitution was unavailable for this study.

We have shown that mosaic, activating substitutions at two residues (p.Asn546Lys and p.Lys656Glu) in the cytoplasmic tyrosine kinase domain of *FGFR1* cause ECCL. The involvement of FGFRs in human disease is well documented.[24,25] Germline gain-of-function mutations in *FGFRs* cause craniosynostosis (*FGFR1-3*)[26–31] and skeletal dysplasia (*FGFR1* and *3*),[32–34] while loss-of-function mutations cause hypogonadotrophic hypogonadism (*FGFR1*, [MIM 615465]) and Hartsfield syndrome (*FGFR1*, [MIM 615465]).[35,36] Lacrimoauriculodentodigital syndrome [MIM 149730] is caused by mutations in *FGFR2*, *FGFR3*, and *FGF10*,[37] and somatic activating mutations in *FGFR3* are present in some epidermal nevi.[38] Both activating mutations and whole gene amplification of *FGFR1* contribute to the pathogenesis of cancer.[24,39] Although activating mutations in the tyrosine kinase domain of *FGFR2* and *FGFR3* have been reported,[25] this is the first report, to our knowledge, of activating mutations in this domain in *FGFR1* associated with a developmental disorder.

Strikingly, the mutations identified in this study in *FGFR1* are paralogous to mutations in *FGFR2* and *FGFR3* that cause craniosynostosis and skeletal dysplasia (Figure 1F).[17,25] The p.Lys650Glu substitution in FGFR3 causes thanatophoric dysplasia II (MIM 187601), and is paralogous to the ECCL-associated p.Lys656Glu substitution in FGFR1.[34] The p.Asn540Lys substitution in FGFR3, paralogous to p.Asn546Lys in FGFR1, is the most common cause of hypochondroplasia (MIM 1460000).[40] Similarly, paralogous substitutions of Asn549 and Lys659 in FGFR2 have been reported in individuals with syndromic craniosynostosis.[41] The identification, in individuals with ECCL, of amino acid substitutions in FGFR1 that are identical to substitutions in other FGF receptors provides additional support for the pathogenicity of these variants, and highlights the distinct roles FGFR1, 2, and 3 signaling during human development.

The findings presented here highlight an emerging link between recurrent somatic activating mutations in tumors and mosaic developmental disorders that frequently have an increased risk of cancer.[42] ECCL represents the first known example of a developmental disorder in the FGFR family with an increased risk for cancer, specifically low-grade gliomas.[8–12] RTKs are one of the most commonly mutated gene families in cancer and their contribution to tumorigenesis is widely recognized.[43] Not surprisingly, both the c.1638C>A (p.Asn546Lys) and c.1966A>G (p.Lys656Glu) mutations in *FGFR1* are known oncogenic mutations,[44–47] and are the two most commonly mutated residues among *FGFR1* mutation-containing tumors in the COSMIC (Catalogue of Somatic Mutations in Cancer) database.[48] Interestingly, most of the tumors associated with substitutions in these two residues are central nervous system gliomas, including pilocytic astrocytomas,[48,49] the same type of tumor seen at increased frequency in individuals with ECCL. In the pilocytic astrocytoma sample from LR12-068, ES identified a second missense substitution, p.Val561Met, also in the tyrosine kinase domain and in *cis* with the p.Lys656Glu substitution. Previous studies have shown that p.Val561Met confers a 38-fold increase in phosphorylation of the FGFR1 receptor, as well as resistance to lucitanib, an FGFR inhibitor currently in phase II clinical trials for FGFR-dependent tumors.[14,15] Whether the p.Val561Met substitution actively contributes to tumorigenesis remains to be elucidated. In individuals with ECCL who develop low-grade gliomas, knowledge of causative *FGFR1* mutations could lead to informed treatment choices with targeted RTK inhibitors and improved clinical management.

The RAS-MAPK pathway regulates crucial cellular processes including DNA synthesis, cell growth, and differentiation. Mutations in components of this pathway cause a variety of developmental syndromes.[50] Oculoectodermal syndrome (OES; [MIM 600268]) is characterized by congenital abnormalities of the scalp (cutis aplasia and focal alopecia) and eyes (eyelid skin tags and epibulbar dermoids), features that are also seen in ECCL.[51] OES has been proposed to be a milder form of ECCL, which is distinguished from OES by the presence of CNS lipomas.[51] Notably, somatic mutations in *KRAS* have recently been associated with OES.[52] Considering the striking phenotypic overlap between ECCL and OES, hyperactive RAS-MAPK signaling might represent a common mechanism underlying these two disorders. The absence of CNS lipomas in OES could be due to the relatively small number of individuals with OES who have had brain imaging, or could reflect the tissue distribution of these somatic mutations. Specific differences in pathway activation due to mutations in *KRAS* versus *FGFR1* might also play a role. Sequencing of *KRAS* in individuals with ECCL, and *FGFR1* in individuals with OES, will be helpful in addressing this question.

In summary, we identified two recurrent mutations in *FGFR1* in individuals with ECCL, a rare neurocutaneous disorder. We developed a smMIP assay to facilitate screening of individuals with suspected ECCL and showed that DNA derived from fibroblasts provides the highest yield for identification of mutations in *FGFR1*. We identified a total of five *FGFR1* individuals with *FGFR1* mutations within our cohort of nine individuals for whom biopsy-derived fibroblast DNA was available. We did not detect any mutations among three individuals for whom only blood- or saliva-derived DNA was available, but this does not rule out the possibility of an *FGFR1* mutation in other tissues. Potential explanations for the individuals in the cohort for whom an *FGFR1* mutation was not detected include (1) mutations present at a level below the limit of detection of our smMIP assay, (2) underlying locus

heterogeneity, and (3) absence of available biopsy-derived DNA for testing. With the exception of the brain tumor from individual LR12-068, all of the samples that possessed an *FGFR1* mutation were from cultured fibroblasts, so that the mutation levels detected might reflect selection for activating *FGFR1* mutations in cell culture. This might explain why the level of mutation in DNA derived from individual LR12-068's brain tumor (32%) is lower than that of his scalp nevus (47%). Sequencing of DNA from uncultured tissue samples from individuals with ECCL will help address this issue. The phenotypes of the individuals without detectable *FGFR1* mutations do not differ significantly from the individuals with *FGFR1* mutations (data not shown). Given the phenotypic similarities between OES and ECCL, screening these individuals for *KRAS* mutations is a logical next step. Our functional analysis of fibroblast cell lines harboring the p.Asn546Lys substitution showed hyperphosphorylation of FGFRs and downstream dependent substrates, consistent with elevated activation of the receptor. Interestingly, elevated FGFR1 signaling is implicated in both proliferation of human mesenchymal stem cells and human preadipocytes and might explain the striking nevus psiloliparus seen in individuals with ECCL.[53,54] We do not currently understand how activating mutations in a single gene can cause ECCL, craniosynostosis, and skeletal dysplasias. It seems likely that the developmental timing and tissue specific location of the post-zygotic *FGFR1* mutation might play an important role. Clearly different activating mutations in *FGFR1* can lead to distinct phenotypes, and further studies are needed to understand the pleiotropic effects of gain-of-function mutations in *FGFR1*. Finally this work adds another gene to the growing number of disorders due to mosaic mutations impacting the RAS-MAPK pathway and further supports the emerging overlap between mosaic developmental disorders and tumorigenesis.

## Supplemental Data

Supplemental Data include five tables and can be found with this article online at http://dx.doi.org/10.1016/j.ajhg.2016.02.006.

## Acknowledgments

We are grateful to the individuals and families who participated in this study. Research reported in this publication was supported by the Care4Rare Canada Consortium (Enhanced Care for Rare Genetic Diseases in Canada) funded by Genome Canada, the Canadian Institutes of Health Research, the Ontario Genomics Institute, Ontario Research Fund, Genome Quebec, and Children's Hospital of Eastern Ontario Foundation; and by the National Institute of Neurological Disorders and Stroke (NINDS) under award numbers 1R01NS092772 (W.B.D.) and the National Human Genome Research Institute of the National Institutes of Health. Some sequencing in this study was provided by the University of Washington Center for Mendelian Genomics (UW-CMG) and was funded by the National Human Genome Research Institute and the National Heart, Lung and Blood Institute grant U54HG006493 to Drs. Debbie Nickerson, Jay Shendure, and Michael Bamshad. M.J.L. and L.G.B. are supported by the Intramural Research Program of the National Human Genome Research Institute. We also acknowledge the contributions of the high-throughput sequencing platform of the McGill University and Genome Quebec Innovation Centre, Montreal, Canada. M.T. received a post-doctoral fellowship from the Reseau de Medecine Genique Appliquee. L.M.M. is supported by a scholarship from the (CIHR) and Consortium National de Formation en Santé. T.Y.T. was supported by an Australian National Health and Medical Research Council Postdoctoral Overseas Training Scholarship (#607431). D.A. and M.O'D. are supported by Cancer Research UK. None of the authors have any conflicts of interest to declare.

Received: November 4, 2015
Accepted: February 9, 2016
Published: March 3, 2016

## Web Resources

The URLs for data presented here are as follows:

COSMIC, http://cancer.sanger.ac.uk/cancergenome/projects/cosmic/
ExAC Browser, http://exac.broadinstitute.org/
Mutalyzer, https://mutalyzer.nl/index
NHLBI Exome Sequencing Project (ESP) Exome Variant Server, http://evs.gs.washington.edu/EVS/
OMIM, http://www.omim.org/
SeattleSeq Annotation 137, http://snp.gs.washington.edu/SeattleSeqAnnotation137/
UCSC Genome Browser, http://genome.ucsc.edu
FGFR1: NM_023110.2

## References

1. Happle, R. (1986). Cutaneous manifestation of lethal genes. Hum. Genet. *72*, 280.
2. Moog, U. (2009). Encephalocraniocutaneous lipomatosis. J. Med. Genet. *46*, 721–729.
3. Hall, J.G. (1988). Review and hypotheses: somatic mosaicism: observations related to clinical genetics. Am. J. Hum. Genet. *43*, 355–363.
4. Hamm, H. (1999). Cutaneous mosaicism of lethal mutations. Am. J. Med. Genet. *85*, 342–345.
5. Happle, R. (1993). Mosaicism in human skin. Understanding the patterns and mechanisms. Arch. Dermatol. *129*, 1460–1470.
6. Hunter, A.G. (2006). Oculocerebrocutaneous and encephalocraniocutaneous lipomatosis syndromes: blind men and an elephant or separate syndromes? Am. J. Med. Genet. A. *140*, 709–726.
7. Moog, U., Jones, M.C., Viskochil, D.H., Verloes, A., Van Allen, M.I., and Dobyns, W.B. (2007). Brain anomalies in encephalocraniocutaneous lipomatosis. Am. J. Med. Genet. A. *143A*, 2963–2972.
8. Bieser, S., Reis, M., Guzman, M., Gauvain, K., Elbabaa, S., Braddock, S.R., and Abdel-Baki, M.S. (2015). Grade II pilocytic astrocytoma in a 3-month-old patient with encephalocraniocutaneous lipomatosis (ECCL): case report and literature review of low grade gliomas in ECCL. Am. J. Med. Genet. A. *167A*, 878–881.

9. Brassesco, M.S., Valera, E.T., Becker, A.P., Castro-Gamero, A.M., de Aboim Machado, A., Santos, A.C., Scrideli, C.A., Oliveira, R.S., Machado, H.R., and Tone, L.G. (2010). Low-grade astrocytoma in a child with encephalocraniocutaneous lipomatosis. J. Neurooncol. *96*, 437–441.
10. Kocak, O., Yarar, C., and Carman, K.B. (2015). Encephalocraniocutaneous lipomatosis, a rare neurocutaneous disorder: report of additional three cases. Childs Nerv. Syst., 1–4. Published online August 1, 2015.
11. Phi, J.H., Park, S.H., Chae, J.H., Wang, K.C., Cho, B.K., and Kim, S.K. (2010). Papillary glioneuronal tumor present in a patient with encephalocraniocutaneous lipomatosis: case report. Neurosurgery *67*, E1165–E1169.
12. Valera, E.T., Brassesco, M.S., Scrideli, C.A., de Castro Barros, M.V., Santos, A.C., Oliveira, R.S., Machado, H.R., and Tone, L.G. (2012). Are patients with encephalocraniocutaneous lipomatosis at increased risk of developing low-grade gliomas? Child's nervous system: ChNS: official journal of the International Society for Pediatric Neurosurgery *28*, 19–22.
13. Moog, U., Roelens, F., Mortier, G.R., Sijstermans, H., Kelly, M., Cox, G.F., Robson, C.D., and Kimonis, V.E. (2007). Encephalocraniocutaneous lipomatosis accompanied by the formation of bone cysts: Harboring clues to pathogenesis? Am. J. Med. Genet. A. *143A*, 2973–2980.
14. Sohl, C.D., Ryan, M.R., Luo, B., Frey, K.M., and Anderson, K.S. (2015). Illuminating the molecular mechanisms of tyrosine kinase inhibitor resistance for the FGFR1 gatekeeper mutation: the Achilles' heel of targeted therapy. ACS Chem. Biol. *10*, 1319–1329.
15. Soria, J.C., DeBraud, F., Bahleda, R., Adamo, B., Andre, F., Dienstmann, R., Delmonte, A., Cereda, R., Isaacson, J., Litten, J., et al. (2014). Phase I/IIa study evaluating the safety, efficacy, pharmacokinetics, and pharmacodynamics of lucitanib in advanced solid tumors. Ann. Oncol. *25*, 2244–2251.
16. Hiatt, J.B., Pritchard, C.C., Salipante, S.J., O'Roak, B.J., and Shendure, J. (2013). Single molecule molecular inversion probes for targeted, high-accuracy detection of low-frequency variation. Genome Res. *23*, 843–854.
17. Beenken, A., and Mohammadi, M. (2009). The FGF family: biology, pathophysiology and therapy. Nat. Rev. Drug Discov. *8*, 235–253.
18. Dorey, K., and Amaya, E. (2010). FGF signalling: diverse roles during early vertebrate embryogenesis. Development *137*, 3731–3742.
19. Mohammadi, M., Olsen, S.K., and Ibrahimi, O.A. (2005). Structural basis for fibroblast growth factor receptor activation. Cytokine Growth Factor Rev. *16*, 107–137.
20. Heldin, C.H. (1995). Dimerization of cell surface receptors in signal transduction. Cell *80*, 213–223.
21. Lemmon, M.A., and Schlessinger, J. (2010). Cell signaling by receptor tyrosine kinases. Cell *141*, 1117–1134.
22. Schlessinger, J. (2000). Cell signaling by receptor tyrosine kinases. Cell *103*, 211–225.
23. Gotoh, N. (2008). Regulation of growth factor signaling by FRS2 family docking/scaffold adaptor proteins. Cancer Sci. *99*, 1319–1325.
24. McDonell, L.M., Kernohan, K.D., Boycott, K.M., and Sawyer, S.L. (2015). Receptor tyrosine kinase mutations in developmental syndromes and cancer: two sides of the same coin. Hum. Mol. Genet. *24* (R1), R60–R66.
25. Wilkie, A.O. (2005). Bad bones, absent smell, selfish testes: the pleiotropic consequences of human FGF receptor mutations. Cytokine Growth Factor Rev. *16*, 187–203.
26. Bellus, G.A., Gaudenz, K., Zackai, E.H., Clarke, L.A., Szabo, J., Francomano, C.A., and Muenke, M. (1996). Identical mutations in three different fibroblast growth factor receptor genes in autosomal dominant craniosynostosis syndromes. Nat. Genet. *14*, 174–176.
27. Jabs, E.W., Li, X., Scott, A.F., Meyers, G., Chen, W., Eccles, M., Mao, J.I., Charnas, L.R., Jackson, C.E., and Jaye, M. (1994). Jackson-Weiss and Crouzon syndromes are allelic with mutations in fibroblast growth factor receptor 2. Nat. Genet. *8*, 275–279.
28. Muenke, M., Gripp, K.W., McDonald-McGinn, D.M., Gaudenz, K., Whitaker, L.A., Bartlett, S.P., Markowitz, R.I., Robin, N.H., Nwokoro, N., Mulvihill, J.J., et al. (1997). A unique point mutation in the fibroblast growth factor receptor 3 gene (FGFR3) defines a new craniosynostosis syndrome. Am. J. Hum. Genet. *60*, 555–564.
29. Muenke, M., Schell, U., Hehr, A., Robin, N.H., Losken, H.W., Schinzel, A., Pulleyn, L.J., Rutland, P., Reardon, W., Malcolm, S., et al. (1994). A common mutation in the fibroblast growth factor receptor 1 gene in Pfeiffer syndrome. Nat. Genet. *8*, 269–274.
30. Reardon, W., Winter, R.M., Rutland, P., Pulleyn, L.J., Jones, B.M., and Malcolm, S. (1994). Mutations in the fibroblast growth factor receptor 2 gene cause Crouzon syndrome. Nat. Genet. *8*, 98–103.
31. Wilkie, A.O., Slaney, S.F., Oldridge, M., Poole, M.D., Ashworth, G.J., Hockley, A.D., Hayward, R.D., David, D.J., Pulleyn, L.J., Rutland, P., et al. (1995). Apert syndrome results from localized mutations of FGFR2 and is allelic with Crouzon syndrome. Nat. Genet. *9*, 165–172.
32. Rousseau, F., Bonaventure, J., Legeai-Mallet, L., Pelet, A., Rozet, J.M., Maroteaux, P., Le Merrer, M., and Munnich, A. (1994). Mutations in the gene encoding fibroblast growth factor receptor-3 in achondroplasia. Nature *371*, 252–254.
33. Shiang, R., Thompson, L.M., Zhu, Y.Z., Church, D.M., Fielder, T.J., Bocian, M., Winokur, S.T., and Wasmuth, J.J. (1994). Mutations in the transmembrane domain of FGFR3 cause the most common genetic form of dwarfism, achondroplasia. Cell *78*, 335–342.
34. Tavormina, P.L., Shiang, R., Thompson, L.M., Zhu, Y.Z., Wilkin, D.J., Lachman, R.S., Wilcox, W.R., Rimoin, D.L., Cohn, D.H., and Wasmuth, J.J. (1995). Thanatophoric dysplasia (types I and II) caused by distinct mutations in fibroblast growth factor receptor 3. Nat. Genet. *9*, 321–328.
35. Dodé, C., Levilliers, J., Dupont, J.M., De Paepe, A., Le Dû, N., Soussi-Yanicostas, N., Coimbra, R.S., Delmaghani, S., Compain-Nouaille, S., Baverel, F., et al. (2003). Loss-of-function mutations in FGFR1 cause autosomal dominant Kallmann syndrome. Nat. Genet. *33*, 463–465.
36. Simonis, N., Migeotte, I., Lambert, N., Perazzolo, C., de Silva, D.C., Dimitrov, B., Heinrichs, C., Janssens, S., Kerr, B., Mortier, G., et al. (2013). FGFR1 mutations cause Hartsfield syndrome, the unique association of holoprosencephaly and ectrodactyly. J. Med. Genet. *50*, 585–592.
37. Rohmann, E., Brunner, H.G., Kayserili, H., Uyguner, O., Nürnberg, G., Lew, E.D., Dobbie, A., Eswarakumar, V.P., Uzumcu, A., Ulubil-Emeroglu, M., et al. (2006). Mutations in different components of FGF signaling in LADD syndrome. Nat. Genet. *38*, 414–417.

38. Hafner, C., Hartmann, A., and Vogt, T. (2007). FGFR3 mutations in epidermal nevi and seborrheic keratoses: lessons from urothelium and skin. J. Invest. Dermatol. *127*, 1572–1573.
39. Weiss, J., Sos, M.L., Seidel, D., Peifer, M., Zander, T., Heuckmann, J.M., Ullrich, R.T., Menon, R., Maier, S., Soltermann, A., et al. (2010). Frequent and focal FGFR1 amplification associates with therapeutically tractable FGFR1 dependency in squamous cell lung cancer. Sci. Transl. Med. *2*, 62ra93.
40. Prinos, P., Costa, T., Sommer, A., Kilpatrick, M.W., and Tsipouras, P. (1995). A common FGFR3 gene mutation in hypochondroplasia. Hum. Mol. Genet. *4*, 2097–2101.
41. Kan, S.H., Elanko, N., Johnson, D., Cornejo-Roldan, L., Cook, J., Reich, E.W., Tomkins, S., Verloes, A., Twigg, S.R., Rannan-Eliya, S., et al. (2002). Genomic screening of fibroblast growth-factor receptor 2 reveals a wide spectrum of mutations in patients with syndromic craniosynostosis. Am. J. Hum. Genet. *70*, 472–486.
42. Bellacosa, A. (2013). Developmental disease and cancer: biological and clinical overlaps. Am. J. Med. Genet. A. *161A*, 2788–2796.
43. Blume-Jensen, P., and Hunter, T. (2001). Oncogenic kinase signalling. Nature *411*, 355–365.
44. Cancer Genome Atlas Research Network (2008). Comprehensive genomic characterization defines human glioblastoma genes and core pathways. Nature *455*, 1061–1068.
45. Hart, K.C., Robertson, S.C., Kanemitsu, M.Y., Meyer, A.N., Tynan, J.A., and Donoghue, D.J. (2000). Transformation and Stat activation by derivatives of FGFR1, FGFR3, and FGFR4. Oncogene *19*, 3309–3320.
46. Lew, E.D., Furdui, C.M., Anderson, K.S., and Schlessinger, J. (2009). The precise sequence of FGF receptor autophosphorylation is kinetically driven and is disrupted by oncogenic mutations. Sci. Signal. *2*, ra6.
47. Rand, V., Huang, J., Stockwell, T., Ferriera, S., Buzko, O., Levy, S., Busam, D., Li, K., Edwards, J.B., Eberhart, C., et al. (2005). Sequence survey of receptor tyrosine kinases reveals mutations in glioblastomas. Proc. Natl. Acad. Sci. USA *102*, 14344–14349.
48. Forbes, S.A., Tang, G., Bindal, N., Bamford, S., Dawson, E., Cole, C., Kok, C.Y., Jia, M., Ewing, R., Menzies, A., et al. (2010). COSMIC (the Catalogue of Somatic Mutations in Cancer): a resource to investigate acquired mutations in human cancer. Nucleic Acids Res. *38*, D652–D657.
49. Jones, D.T., Hutter, B., Jäger, N., Korshunov, A., Kool, M., Warnatz, H.J., Zichner, T., Lambert, S.R., Ryzhova, M., Quang, D.A., et al.; International Cancer Genome Consortium PedBrain Tumor Project (2013). Recurrent somatic alterations of FGFR1 and NTRK2 in pilocytic astrocytoma. Nat. Genet. *45*, 927–932.
50. Schubbert, S., Shannon, K., and Bollag, G. (2007). Hyperactive Ras in developmental disorders and cancer. Nat. Rev. Cancer *7*, 295–308.
51. Ardinger, H.H., Horii, K.A., and Begleiter, M.L. (2007). Expanding the phenotype of oculoectodermal syndrome: possible relationship to encephalocraniocutaneous lipomatosis. Am. J. Med. Genet. A. *143A*, 2959–2962.
52. Peacock, J.D., Dykema, K.J., Toriello, H.V., Mooney, M.R., Scholten, D.J., 2nd, Winn, M.E., Borgman, A., Duesbery, N.S., Hiemenga, J.A., Liu, C., et al. (2015). Oculoectodermal syndrome is a mosaic RASopathy associated with KRAS alterations. Am. J. Med. Genet. A. *167*, 1429–1435.
53. Dombrowski, C., Helledie, T., Ling, L., Grünert, M., Canning, C.A., Jones, C.M., Hui, J.H., Nurcombe, V., van Wijnen, A.J., and Cool, S.M. (2013). FGFR1 signaling stimulates proliferation of human mesenchymal stem cells by inhibiting the cyclin-dependent kinase inhibitors p21(Waf1) and p27(Kip1). Stem Cells *31*, 2724–2736.
54. Widberg, C.H., Newell, F.S., Bachmann, A.W., Ramnoruth, S.N., Spelta, M.C., Whitehead, J.P., Hutley, L.J., and Prins, J.B. (2009). Fibroblast growth factor receptor 1 is a key regulator of early adipogenic events in human preadipocytes. Am. J. Physiol. Endocrinol. Metab. *296*, E121–E131.
55. Kearse, M., Moir, R., Wilson, A., Stones-Havas, S., Cheung, M., Sturrock, S., Buxton, S., Cooper, A., Markowitz, S., Duran, C., et al. (2012). Geneious Basic: an integrated and extendable desktop software platform for the organization and analysis of sequence data. Bioinformatics *28*, 1647–1649.
56. Wilkie, A.O., Bochukova, E.G., Hansen, R.M., Taylor, I.B., Rannan-Eliya, S.V., Byren, J.C., Wall, S.A., Ramos, L., Venâncio, M., Hurst, J.A., et al. (2006). Clinical dividends from the molecular genetic diagnosis of craniosynostosis. Am. J. Med. Genet. A. *140*, 2631–2639.
57. Berk, D.R., Spector, E.B., and Bayliss, S.J. (2007). Familial acanthosis nigricans due to K650T FGFR3 mutation. Arch. Dermatol. *143*, 1153–1156.
58. Wilcox, W.R., Tavormina, P.L., Krakow, D., Kitoh, H., Lachman, R.S., Wasmuth, J.J., Thompson, L.M., and Rimoin, D.L. (1998). Molecular, radiologic, and histopathologic correlations in thanatophoric dysplasia. Am. J. Med. Genet. *78*, 274–281.
59. Nowaczyk, M.J., Mernagh, J.R., Bourgeois, J.M., Thompson, P.J., and Jurriaans, E. (2000). Antenatal and postnatal findings in encephalocraniocutaneous lipomatosis. Am. J. Med. Genet. *91*, 261–266.
60. Kupsik, M., and Brandling-Bennett, H. (2013). An infant with an alopecic plaque on the scalp and ocular choristomas: case presentation. Diagnosis: Encephalocraniocutaneous lipomatosis (ECCL). Pediatr. Dermatol. *30*, 491–492.

**The American Journal of Human Genetics, Volume *98***

## Supplemental Information

# Mosaic Activating Mutations in *FGFR1* Cause Encephalocraniocutaneous Lipomatosis

**James T. Bennett, Tiong Yang Tan, Diana Alcantara, Martine Tétrault, Andrew E. Timms, Dana Jensen, Sarah Collins, Malgorzata J.M. Nowaczyk, Marjorie J. Lindhurst, Katherine M. Christensen, Stephen R. Braddock, Heather Brandling-Bennett, Raoul C.M. Hennekam, Brian Chung, Anna Lehman, John Su, SuYuen Ng, David J. Amor, Jacek Majewski, Les G. Biesecker, Kym M. Boycott, William B. Dobyns, Mark O'Driscoll, Ute Moog, Laura M. McDonell, University of Washington Center for Mendelian Genomics, and Care4Rare Canada Consortium**

## SUPPLEMENTAL DATA

**TABLE S1**. Capture methods and coverage summary of exome data

| | LR12-068 | | LR13-278 | | | LR13-175 | | IN_0039 | | NIH_183 | |
|---|---|---|---|---|---|---|---|---|---|---|---|
| | Tumor* | Scalp nevus | Unaffected skin | Scalp nevus | Eyelid dermoid | Scalp nevus | Lipoma | Scalp nevus | Unaffected skin | Scalp nevus | Blood* |
| **Capture Method** | SeqCap EZ Exome Library v2.0 kit | | | | | | | SureSelect All Exon V5 | | SeqCap EX Exome+UTR | |
| **Mean Coverage** | 122X | 160X | 161X | 160X | 150X | 169X | 172X | 106X | 105X | 65X | 64X |
| **% Covered > 20X** | 95.9 | 97.7 | 97.3 | 97.1 | 96.6 | 97.8 | 97.9 | 94.7 | 94.7 | 83.1 | 84.4 |
| **c.1638C>A (p.Asn546Lys)** | 0% (47) | 0% (98) | 35% (74) | 42% (99) | 54% (92) | 0% (93) | 0% (105) | 33% (76) | 23% (61) | 0% (24) | 0% (39) |
| **c.1966A>G (p.Lys656Glu)** | 32% (127) | 47% (182) | 0% (219) | 0% (172) | 0% (181) | 0% (202) | 0% (205) | 0% (70) | 0% (90) | 45% (29) | 0% (40) |

All DNA isolated from cultured fibroblasts cultured from biopsied tissue except those with asterisk (*), in which DNA was directly isolated from tissue without culture.

**TABLE S2:** Exome sequencing and variant filtering pipelines

| *Sample* | **LR12-068, LR13-278, LR13-175** | **IN_0039** | **NIH_183** |
|---|---|---|---|
| *Sequencing platform* | HiSeq 2000 (Illumina) | HiSeq 2000 (Illumina) | HiSeq 2500 (Illumina) |
| *Sequence alignment* | Burrows-Wheeler Aligner | Burrows-Wheeler Aligner | Novoalign |
| *Variant calling & annotation* | Unified Genotyper, SeattleSeq Annotation Server | GATK, SAMtools, BCFtools, custom script | Shimmer, Mutect, Somatic Sniper |
| *Filtering* | missense,nonsense, & splice variants with < 1% in EVS, ExAC, & dbSNP | missense,nonsense, & splice variants with < 1% in EVS, ExAC, & dbSNP. Not seen in > 5 in-house exomes | missense, nonsense and splice variants with < 2% ClinSeq™ frequency* |

*ClinSeq™ frequency is defined as the number of individuals with alternative allele frequency ≥1%, divided by the number of individuals with at least ten reads at that position. This is a population frequency based filter that is not limited to constitutional variants (as is the case with EVS, EXAC, and dbSNP), and is based on the NIH in house ClinSeq dataset (www.genome.gov/25521305)

**TABLE S3:** Primers used for subcloning 1408 basepair fragment containing c.1681G>A (p.Val561Met) and c.1966A>G (p.Lys656Glu)

| **Name** | **Sequence** |
|---|---|
| FGFR1_ex14_F | CTTTGAGGTGAAGCCAAACC |
| FGFR1_ex15_R | ACCCCACTCCTTGCTTCTC |

**TABLE S4**: Sequences for *FGFR1* smMIPs

| Name | Sequence |
|---|---|
| FGFR1_01 | GAGCTCTGGCTCTGGCACGGGCTTCAGCTTCCCGATATCCGACGGTAGTGTNNNNNGGGTGTCGGGAAAGCTGGGGG |
| FGFR1_02 | CACGCCCTCCCCAGACTCCACTTCAGCTTCCCGATATCCGACGGTAGTGTNNNNNTTTCCCGACACCCGGAGCTCTACGT |
| FGFR1_03 | GGGCCCCTCCTCCCTGCTCAGGGAGGTGCTTCAGCTTCCCGATATCCGACGGTAGTGTNNNNNATGAGAGAAGACGGAA |
| FGFR1_04 | CCCACTGCGTGCACGCACCTTCAGCTTCCCGATATCCGACGGTAGTGTNNNNNGTACATGATGATGCGGGACTGCTGGC |
| FGFR1_05 | CGTCTCCTGGAGATGGATACTCTCTAGTCCTTCAGCTTCCCGATATCCGACGGTAGTGTNNNNNCCTGGTTGGAGGTCAA |
| FGFR1_06 | GCAAATGGGCGGAGAGCCACAGGGTGTTACTTCAGCTTCCCGATATCCGACGGTAGTGTNNNNNTGGTGCAGTTACTGGG |
| FGFR1_07 | TGAGCCAGGCCTTGGGGCACTTCAGCTTCCCGATATCCGACGGTAGTGTNNNNNTGGGAGATCTTCACTCTGGGCGG |
| FGFR1_08 | CGCATGGACAAGCCCAGTAACTGCACCAACTTCAGCTTCCCGATATCCGACGGTAGTGTNNNNNAACACCCTGTGGCTCT |
| FGFR1_09 | TGGCCCCAGGCAGGGCCATGACTTCAGCTTCCCGATATCCGACGGTAGTGTNNNNNTCTCTATCCCACACCTCCCTGGCA |
| FGFR1_10 | CCTCTGTCACCAGGACATTCCTGGCTGCCCTTCAGCTTCCCGATATCCGACGGTAGTGTNNNNNCACTCCTTGCTTCTCA |
| FGFR1_11 | CGCACGGGACATTCACCACATCGACTACTTCAGCTTCCCGATATCCGACGGTAGTGTNNNNNCAGAGCCTTCCAGCTC |
| FGFR1_12 | GGGTTGTGGCTGGGGTTGTCTTCAGCTTCCCGATATCCGACGGTAGTGTNNNNNAAGACTAGGGGGGCTCTGTTCCCAC |
| FGFR1_13 | AGCAGCTCTCCTCCAAGGACCTGGTGTCCCTTCAGCTTCCCGATATCCGACGGTAGTGTNNNNNTCTTCTCCTGTGCCTG |
| FGFR1_14 | CCACCCCCAGCAGCACACCCTTCAGCTTCCCGATATCCGACGGTAGTGTNNNNNGGGGCCTCCGGGCCTGCAGGTACTCC |
| FGFR1_15 | GCTAGGGAAGGGGGTTAAGAGAGGCTGCTTCAGCTTCCCGATATCCGACGGTAGTGTNNNNNGGGAAGCATAAGAATA |
| FGFR1_16 | CGCAGGATGGTGGGTGCCGGCCAGACTGCTTCAGCTTCCCGATATCCGACGGTAGTGTNNNNNCAAGTAAATGAGTCTCA |
| FGFR1_17 | CCCATTCCAAGCAAACAGCAGGCCTTCAGCTTCCCGATATCCGACGGTAGTGTNNNNNTGGGAGAGGGCTGCTTTGGG |
| FGFR1_18 | CGTGTGACCAAAGTGGCTGTGAAGATGTCTTCAGCTTCCCGATATCCGACGGTAGTGTNNNNNAACTTCACCAGCCCCAA |
| FGFR1_19 | CGAACCAGAAGAACCCCAGAGTTCATGGACTTCAGCTTCCCGATATCCGACGGTAGTGTNNNNNAATGCCTTCAAAAAGT |
| FGFR1_20 | GCAAGGAGGGGGGACGGGGTGACTCCTCTTCAGCTTCCCGATATCCGACGGTAGTGTNNNNNTCATACTCAGAGACCC |
| FGFR1_21 | TGCACACTCAGCACCACCCTTCAGCTTCCCGATATCCGACGGTAGTGTNNNNNATCTCCTGCATGGTGGGGTCGGTCATC |
| FGFR1_22 | GGTACCAAGAAGAGTGACTTCCACAGCCACTTCAGCTTCCCGATATCCGACGGTAGTGTNNNNNCACTGACTCAGCCCTG |
| FGFR1_23_SNPa | AGGCC**G**GCAGTGATGACCTCGCCCCTGTACTTCAGCTTCCCGATATCCGACGGTAGTGTNNNNNCATGGTTCTTCTCCCT |
| FGFR1_23_SNPb | AGGCC**A**GCAGTGATGACCTCGCCCCTGTACTTCAGCTTCCCGATATCCGACGGTAGTGTNNNNNCATGGTTCTTCTCCCT |
| FGFR1_24_SNPa | CGTGCC**C**GTGGCGAGGGCAGGACATCTTCAGCTTCCCGATATCCGACGGTAGTGTNNNNNCTAGGGAAGCTCTTCTC |
| FGFR1_24_SNPb | CGTGCC**T**GTGGCGAGGGCAGGACATCTTCAGCTTCCCGATATCCGACGGTAGTGTNNNNNCTAGGGAAGCTCTTCTC |
| FGFR1_25 | GGGGAGACACAGAGGCAGGAGAGCTGCTTCAGCTTCCCGATATCCGACGGTAGTGTNNNNNGTGCTTGGCGGGTAAC |
| FGFR1_26 | CGGAAGCAAAATGGACAAGCACAGGACCTTCAGCTTCCCGATATCCGACGGTAGTGTNNNNNGAGTGATGGGAGAGTC |
| FGFR1_27 | CGTCACTGGGGCTTTGGGGTCAGCTACACTTCAGCTTCCCGATATCCGACGGTAGTGTNNNNNACACACACTCCATCTCA |
| FGFR1_28 | AGTAACAGAGGTCACAAAGTGGAGGTGAGCTTCAGCTTCCCGATATCCGACGGTAGTGTNNNNNTGGGAAGGAGACCACT |
| FGFR1_29 | CGGGGGCTCAAGTTCCTGTGGGCAGCTTCAGCTTCCCGATATCCGACGGTAGTGTNNNNNGCACATCCAGTGGCTAAAG |
| FGFR1_30 | CGGTGAGGGGACCGCTCTGTGGACTTCAGCTTCCCGATATCCGACGGTAGTGTNNNNNAATCTTGCTCCCATTCACCTC |
| FGFR1_31 | GGGTGGGCTCACCTGCGCCTTCAGCTTCCCGATATCCGACGGTAGTGTNNNNNTTACACATGAACTCCACGTTGCTACC |
| FGFR1_32 | AAGAGCCAGGCTTGGAGAACACAGCCCTTCAGCTTCCCGATATCCGACGGTAGTGTNNNNNTGGACTCTGTGGTGCCCT |
| FGFR1_33 | GGCAACTACACCTGCATTGTGGAGACTTCAGCTTCCCGATATCCGACGGTAGTGTNNNNNAGGTGCCACGGGGTGC |
| FGFR1_34 | AGGGGAGGCCGAGTTAGGAAGTCCTGATTCTTCAGCTTCCCGATATCCGACGGTAGTGTNNNNNCAAATGCCCTTCCAGT |
| FGFR1_35 | GGGACCCCAAACCCCACACCTTCAGCTTCCCGATATCCGACGGTAGTGTNNNNNAGCTGCTCCTCTCCACCCTGCCT |
| FGFR1_36 | GGGAAGAAGAAGGGGCACTGAGGTTCCTCCTTCAGCTTCCCGATATCCGACGGTAGTGTNNNNNCAGACCCAAAGGGCAG |
| FGFR1_37 | GGACACCCTCCCCATGGGGATCTTCAGCTTCCCGATATCCGACGGTAGTGTNNNNNTTTCTCCTCTGAAGAGGAGTCA |
| FGFR1_38_SNPa | GGGCAC**G**GAGTCCTGCACCTCCTTCAGCTTCCCGATATCCGACGGTAGTGTNNNNNTGGCAGAGAGGGCTGGAGGGGG |
| FGFR1_38_SNPb | GGGCAC**A**GAGTCCTGCACCTCCTTCAGCTTCCCGATATCCGACGGTAGTGTNNNNNTGGCAGAGAGGGCTGGAGGGGG |
| FGFR1_39 | TGCTCTGCACATCGTCCCCTTCAGCTTCCCGATATCCGACGGTAGTGTNNNNNTGGTGTCACTGCCCGAGGGGCTGCTG |
| FGFR1_40 | TCAACTGGCTGCGGGACGCTTCAGCTTCCCGATATCCGACGGTAGTGTNNNNNTCTCTCGCCCCTTGGCTTCCCTTC |
| FGFR1_41 | CGTAATAAAAAAACCTCTGCAGAGGGCCCCTTCAGCTTCCCGATATCCGACGGTAGTGTNNNNNTTTTGGGGCTCTCTCC |
| FGFR1_42 | GGGCAGCCTGGACTCCTGGGCCTTGGGACTTCAGCTTCCCGATATCCGACGGTAGTGTNNNNNTCACCAACCTCTAACT |
| FGFR1_43 | GGATGTGGAGCTGGAAGTGCCTCCTCTCTTCAGCTTCCCGATATCCGACGGTAGTGTNNNNNTCCCCTACCTAGACCCT |
| FGFR1_44 | CCCTCTGATGAGTGGGAAACTGAGATGTGCTTCAGCTTCCCGATATCCGACGGTAGTGTNNNNNCTATCTCACCAGACAC |

Sequences of all 47 smMIPs used in this study are listed. The string of five N's represents the degenerate molecular tag. Three smMIPs overlapped a common SNP, so smMIPs complimentary to both alleles (in red) were used, and labeled "a" and "b"

**TABLE S5:** Coverage depth at the two *FGFR1* mutation sites for each sample sequenced by smMIPs

| Cohort | Individual | Tissue | c.1638C>A (p.Asn546Lys) | c.1966A>G (p.Lys656Glu) |
|---|---|---|---|---|
| **Exome sequencing** | **LR13-278** | Unaffected Skin | 50/160 (31%) | 0/22 |
| | | Scalp Nevus | 52/108 (48%) | 0/12 |
| | | Eyelid Dermoid | 42/76 (55%) | low coverage |
| | | Blood | 0/153 | 0/29 |
| | | Saliva | 0/27 | 0/28 |
| | **IN_0039** | Scalp Nevus | 30/83 (36%) | low coverage |
| | | Saliva | 0/114 | low coverage |
| | | Buccal | 0/40 | low coverage |
| | | Blood | 0/51 | low coverage |
| **Tissue biopsy available** | **LR14-261** | Scalp Nevus | 110/199 (55%) | 0/67 |
| | | Saliva | 0/36 | low coverage |
| | **LR04-090** | Unaffected skin | 0/119 | 0/22 |
| | | Saliva | 0/228 | 0/36 |
| | | Blood | 0/119 | 0/23 |
| | **LR09-120** | Scalp Nevus | 0/35 | 0/19 |
| | | Saliva | 0/124 | 0/24 |
| | **IN_0025** | Lipoma | 0/117 | 0/22 |
| | | Blood | 0/211 | 0/26 |
| | | Saliva | 0/94 | 0/25 |
| **Blood/Saliva Only** | **LR04-093** | Blood | 0/152 | 0/39 |
| | **LR09-252** | Saliva | 0/105 | 0/28 |
| | **LR14-210** | Blood | 0/227 | 0/49 |

Low coverage was defined as less than 10 independent reads